Dear Editor,

Thank you for evaluating our manuscript and considering it for publication in NHESS. We have taken note of all the reviewers' comments and appreciate them. We have also taken the opportunity to further clarify and improve some aspects of the manuscript. The subsequent pages address the changes, clarifications and improvements according to the following notation: text in bold refers to comments from the editor or reviewers, text in normal black font refers to replies to these comments and text in italics refers to new text added in the manuscript.

Editor

Having carefully considered the reviewers' recommendations and the authors' response, I am pleased to inform you that your manuscript has been deemed suitable for publication pending a minor revision.

The reviewers found your work to be of interest to the readership and acknowledged its contribution to the field of coastal hazards. The required revisions are straightforward, primarily involving clarification of specific terms and correction of minor grammatical errors.

The authors would like to thank Dr. Gao and the three anonymous reviewers for their thorough and careful revision of the manuscript. We believe the manuscript has significantly improved as a result of their feedback. The main revisions carried out in response to the reviewers' comments are:

- A new section dedicated to the application of the methodology to two real-world study areas along the southern Iberian Peninsula, using previously calibrated and validated models incorporating real-world drivers.
- A comprehensive sensitivity analysis of key model parameters (eddy viscosity and bed roughness), demonstrating the robustness of the optimal POT combination with respect to numerical settings.
- An expanded Discussion section, including a major revision of Section 6.3 (formerly 5.3) "Limitations and further improvements", with a clearer distinction between limitations of the numerical model and limitations intrinsic to the LWP-based methodology.
- The inclusion of the Longshore vs. Cross-shore (LvC) index, proposed by López-Doriga & Ferreira (2017)[1], which provides a physically based framework for interpreting the relative performance of LWP and Hs across different wave climate conditions.

Additionally, as detailed in the responses to Reviewers 2 and 3, a sensitivity analysis of sediment grain size was conducted using D50 = 0.5 mm and D50 = 2 mm as alternatives to the original D50 = 1 mm. The results confirm that the optimal POT combination is maintained across all grain size scenarios. Given the current length of the manuscript and the addition of the new section featuring real-world data, we have decided to omit these specific results to maintain conciseness.

[1] López-Dóriga, U. and Ferreira, Ó.: Longshore and cross-shore morphological variability of a berm-bar system under low to moderate wave energy, J Coast Res, 33, 1161–1171, https://doi.org/10.2112/JCOASTRES-D-16-00050.1, 2017.

Anonymous Referee #1

This study defines optimized Peak Over Threshold (POT) parameters and utilizing Longitudinal Wave Power (LWP) to identify significant morphological changes. The authors employed the Delft3D numerical model to simulate the morphological evolution of an idealized river mouth. This is an interesting work. However, there are some concerns regarding the absence of field validation, the significant simplification of model assumptions, and a potential over-reliance on specific parameters. Therefore, I recommend a Major Revision. Potentially useful suggestions are listed below:

The authors sincerely thank Reviewer 1 for their careful reading and insightful comments on our manuscript. In response to their suggestions, we have performed a sensitivity analysis as requested and revised and improved the manuscript accordingly.

Moreover, following the reviewers' suggestions, a new section has been incorporated into the manuscript to present the application of the methodology to two real-world study areas. These applications were carried out using previously calibrated and validated numerical models, whose calibration and validation were performed against real measured bathymetric data. This provides a meaningful empirical grounding for the methodology beyond the idealized framework, while also introducing real-world forcings including observed wave conditions, complete tidal regimes, and variable river discharges, and also different sediment grain sizes. As shown in the revised manuscript, the new Section 5, "Application to real-world study areas", reads as follows:

"*The methodology was applied to two different real-world study areas: the Punta Umbría Inlet, following Zarzuelo et al. (2019) and the Guadiana estuary, following López-Ruiz et al. (2020). For both study cases, models were implemented in Delft3D and have been calibrated and validated against field-measured bathymetric surveys, providing continuous morphological simulations over real observed periods. For the Punta Umbría Inlet, the model spans from July 2014 to October 2015, with model data obtained at 3-hour intervals. For the Guadiana estuary, two separate simulations with hourly data were utilized: (1) from July 2016 to June 2017, and (2) from June 2017 to December 2018. This section presents the match results for each simulation using the two primary POT combinations: T-POT and Combination 11.*

5.1. Punta Umbría Inlet

The Punta Umbría Inlet (hereinafter PUI) consists of a NW-SE trending channel, 8 km in length and 0.5 km in width, with a maximum depth of -12 m MSL. Characterized as an ebb-tidal system, it features minor ebb channels, shoals, and frontal lobes. The model utilizes a spatially distributed D50 sediment grain size, ranging from 0.5 to 4 mm. This is defined via a grid-based input file to reflect the natural variability of the seabed. Due to long-standing navigational difficulties associated with shoal development, a jetty was constructed at the inlet, reaching -4 m MSL. The numerical setup and validation procedures follow Zarzuelo et al. (2019) in their entirety. A comprehensive description of the model performance is available in that study.

The control volume used to apply the methodology is located in the channel (Figure S11 from Supplementary Material). The match values obtained for the T-POT are 43.4% and 41.4% for the LWP-ME90 and LWP-ME95, respectively, and 42,7% and 45,1% for the Hs-ME90 and Hs-ME95,

respectively. For the optimal combination (Combination 11, POT(95,4,6)), the match results for LWP increase to 47.4% (ME90) and 47.5% (ME95), while the Hs matches remain identical to those of the T-POT. This suggests that the Combination 11 improves upon the T-POT for LWP while maintaining the same accuracy for Hs.

5.2. Guadiana estuary

The numerical setup for the Guadiana estuary follows the configuration described in López-Ruiz et al. (2020), where a comprehensive description of the model's calibration and performance is available. The study area encompasses the ebb-tidal delta of the Guadiana River, located at the southern border between Spain and Portugal. The region is characterized by a semi-diurnal mesotidal regime, with a mean tidal range of 2 m. Similar to the PUI, the river mouth is stabilized by a jetty system, and the main channel undergoes periodic dredging to maintain navigability. Sediment distribution in the area exhibits the high variability typical of deltaic environments, with grain sizes ranging from fine to coarse sands. The model utilizes a spatially distributed D50 sediment grain size, ranging from 1 to 10 mm. This is defined via a grid-based input file to reflect the natural variability of the seabed.

Two simulations covering different periods are available for this study area, hereafter referred to as Guadiana 1617 (from July 2016 to June 2017) and Guadiana 1718 (from June 2017 to December 2018). The control volume used to apply the methodology is located in the ebb delta, within an area comparable to the one analyzed by Garel et al. (2019) to unravel the sediment transport patterns in the delta (Figure S12 from Supplementary Material).

For Guadiana 1617, the match values obtained for the T-POT are 63.5% and 62.9% for the LWP-ME90 and LWP-ME95, respectively, and 64.3% and 63.9% for the Hs-ME90 and Hs-ME95, respectively. For the Combination 11, the match results for LWP increase to 67.5% (ME90) and 67.9% (ME95), while the Hs matches remain identical to those of the T-POT.

For the Guadiana 1718 period, the T-POT achieved match values of 72.3% and 90.5% for LWP (ME90 and ME95, respectively), and 73.1% and 90.5% for Hs. The Combination 11 improved the LWP-ME90 match to 79% and the Hs-ME90 to 74.4%, while maintaining identical results for all ME95 events. Notably, almost all ME95 occurred during Storm Emma (February 2018), which heavily impacted the South Atlantic coast of the Iberian Peninsula (Málvarez et al. 2021)."

As demonstrated, the application to real-world scenarios confirms the robustness of the methodology. The optimal POT combination (Combination 11) consistently outperforms the T-POT across the three simulations analyzed regarding LWP matches. The single exception is the Guadiana 1718 case, where the dominance of a single extreme event (Storm Emma) concentrates nearly all ME95 events within a brief period, thereby limiting the discriminatory capacity of the LWP-based proxy under such specific conditions. This behavior is consistent with the role of the LvC index discussed in Section 6.1 of the revised manuscript (and further detailed in our response to Comment 1), reinforcing the complementary nature of LWP and Hs as morphological proxies. Moreover, the Hs related matches for the optimal POT combination are equal to the T-POT matches, with the exception of Guadiana 1718, where the match for Hs-ME90 shows an improvement over the T-POT.

Storm Emma (February 28 – March 5, 2018) was a severe Atlantic event that triggered extreme meteorological and oceanographic conditions across the southwestern Iberian Peninsula. It produced

a 22-year record significant wave height of 7.27 m and raised sea levels to 4.12 m through a combination of low atmospheric pressure and spring tides. These forces caused profound morphodynamic changes, including dune erosion of 2.5 m and the modification of seabed elevation at depths as great as -10 m (García-de-Lomas, et al., 2019; Málvarez et al. 2021).

The Figures S11 and S12 from the Supplementary Material correspond to Figure 1 and Figure 2, respectively, from the present document.

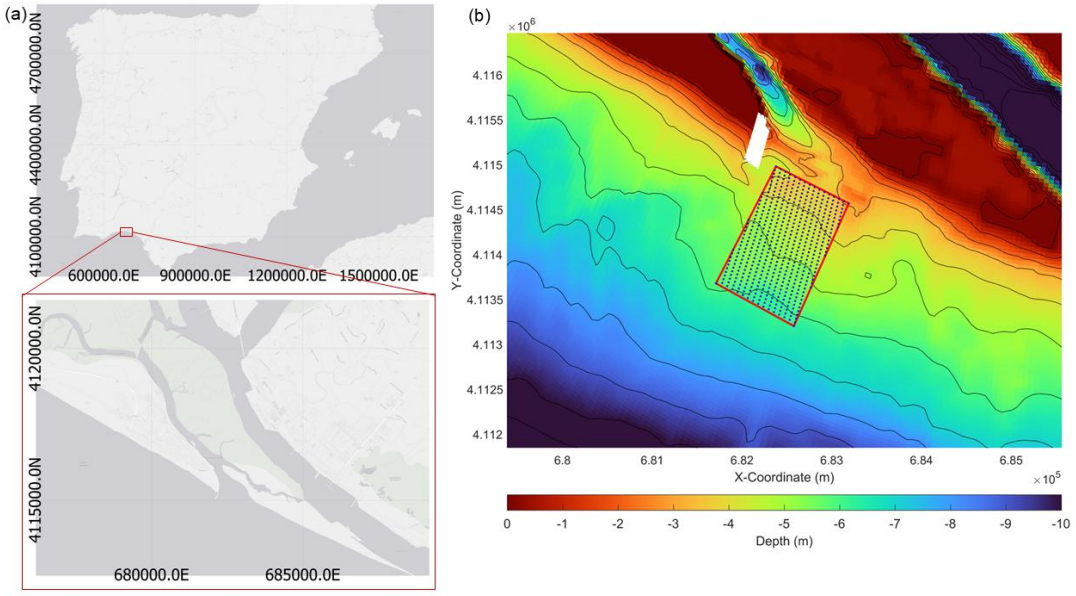

Figure 1. (a) Study area location in the Iberian Peninsula. (b) Control volume for the Punta Umbría Inlet shown on the actual bathymetry of the area. Bathymetric contours are represented every 1m, from 0 to -12 m MSL.

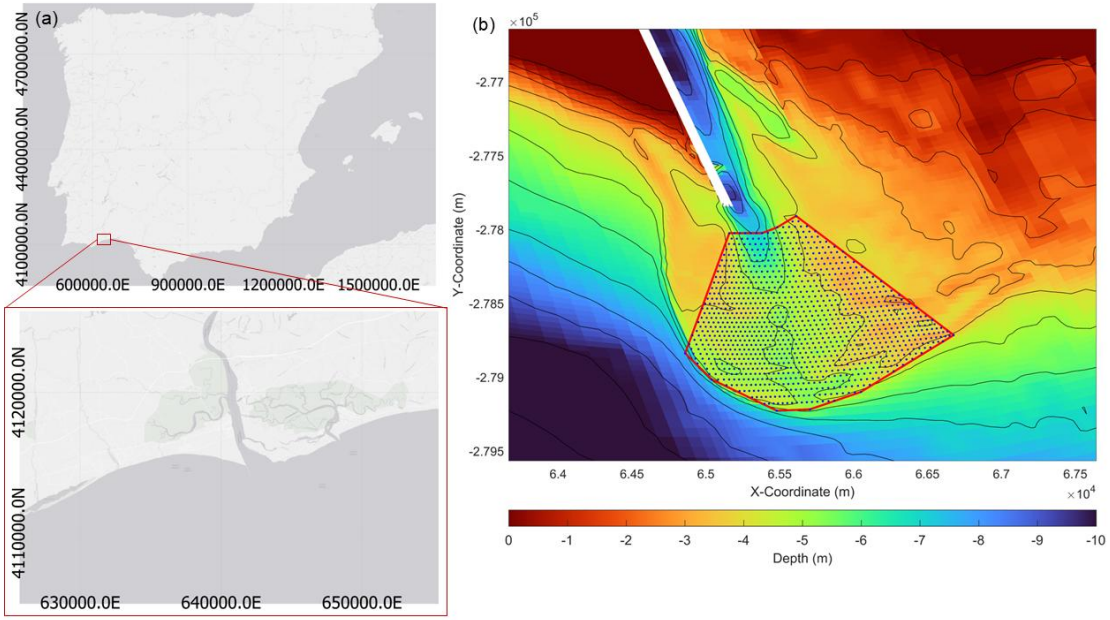

Figure 2. (a) Study area location in the Iberian Peninsula. (b) Control volume for the Guadiana Estuary shown on the actual bathymetry of the area. Bathymetric contours are represented every 1 m, from 0 to -12 m MSL.

1. **While the authors have cited extensive literature on storm erosion, there appears to be limited discussion on existing studies that also utilize Wave Power or Energy Flux for prediction purposes. Expanding this section would strengthen the context.**

Following the reviewer's recommendation, the Introduction and Section 6.1 (formerly Section 5.1) have been updated to include additional references on the use of Wave Energy Flux and Wave Power in coastal risk assessment, and to demonstrate how they align with the methodology proposed in this study.

Recent literature has increasingly adopted Wave Energy Flux (WEF) and Wave Power as fundamental metrics in coastal risk evaluation. Mentaschi et al. (2017) utilize the 100-year return level of WEF as a robust proxy for both coastal flooding and erosion. This approach is supported by the work of Pinson et al. (2012), who emphasize that because WEF represents the actual power available in the sea, it is the central variable for understanding the physical stress applied to the coastal environment. More recently, Rusu (2022) demonstrated that the spatial distribution of wave power is heavily influenced by local bathymetry, highlighting its relevance for site-specific coastal planning.

In line with this body of literature, a relationship between wave energy and sediment transport can be further quantified to distinguish the specific nature of coastal changes. López-Dóriga and Ferreira (2017) proposed the Longshore vs. Cross-shore (LvC) index, which relates wave energy conditions to volumetric sediment changes to determine whether a storm event or coastal area is longshore-dominated or cross-shore-dominated. This index has been incorporated into the present study in section 6.1 "The role of wave direction" (formerly Section 5.1) of the revised manuscript, reading as follows: "*Furthermore, by applying the LvC (Longshore vs. Cross-shore) index proposed by López-Dóriga and Ferreira (2017), it was found that the NCV exhibits a more cross-shore dominated in experiment 2 (1990-91) with an LvC=0.18, and in experiment 5 (2010-11) with LvC=0.01, both of which correspond to a higher H_s-match. Conversely, the SCV shows systematically higher LvC across most experiment, indicating a greater degree of longshore dominance, which corresponds with a higher LWP-match. The calculated LvC indices for all experiments and control volumes are provided in Table S5 of the Supplementary Material.*"

Table S5 from the Supplementary Material corresponds to Table 1 of the present document.

Table 1. LvC index calculated for each CV and for each experiment.

Year (Experiment)	NCV	SCV
1980-1981 (1)	0.25	0.30
1990-1991 (2)	0.18	0.60
1999-2000 (3)	0.85	0.66
2000-2001 (4)	0.38	0.44
2010-2011 (5)	0.01	0.40
2019-2020 (6)	0.17	0.75

Additionally, the text added in the Introduction reads as follows: *"Furthermore, some studies have employed the Wave Energy Flux or the Wave Power for coastal risk evaluation. For instance, in Mentaschi et al. (2017), where they use the 100-year return level of Wave Energy Flux as a robust*

proxy for both coastal flooding and erosion. More recently, Rusu (2022) demonstrated that the spatial distribution of wave power is heavily influenced by local bathymetry, highlighting its relevance for site-specific coastal planning"

2. **It is recommended that the authors also highlight the DEFICIENCIES OF EXISTING STATISTICAL METHODs, rather than solely focusing on the neglect of physical processes.**

We thank the reviewer for this suggestion. The POT methodology was originally developed to improve upon the Annual Maxima Method (AMM), which assumes that annual maximum values are independent and identically distributed. A significant limitation of the AMM is its reliance on a single value per year, whereas the POT method allows for the inclusion of multiple extreme events (Mendez et al. 2006). Therefore, the POT model utilizes a sample of major storms considerably larger than the number of annual maxima.

However, the deficiencies of the POT method primarily relate to parameter selection. As noted by Almarshed (2025), the selection of an appropriate threshold must balance two competing requirements: it must be high enough to ensure the statistical independence of events, yet not so restrictive as to exclude a significant number of relevant extremes. This trade-off is inherently context-specific, as POT parameters vary across different geographic regions and wave climate conditions.

The POT methodology is widely used. However, the importance of site-specific parameters is a key consideration already addressed in the manuscript. As stated in the manuscript (Section 3): *"Even though coastal storm thresholds are site-specific (Harley, 2017), the existing literature lacks a unified criterion for these parameters even within the same geographical regions. Storm definitions are commonly different between authors, and storm thresholds are often selected arbitrarily, with the statistical and meteorological independence between storm events frequently being neglected (Kummerer et al., 2024). This non-uniformity is evident in the threshold selection: for instance, studies on the Mediterranean Sea utilize varying wave height thresholds, such as the 95th percentile (Martzikos et al., 2021), 96th percentile (Del-Rosal-Salido et al., 2025), or 98th percentile (Sanuy et al., 2024).*

Similarly, the minimum storm duration exhibits significant regional variability: it ranges from 6 hours (Mendoza et al., 2011) to 12 hours (Ojeda et al., 2017) for the Mediterranean Sea, while on the Atlantic coast (Portugal and West Andalusia), the range is even wider, varying from 12 hours (Puig et al., 2016) to 48 hours (Almeida et al., 2012). Regarding the independence criterion, which is typically approached using a fixed value (Martzikos et al., 2021), the values shown in Table 2 were selected to cover the observed range in literature. This range extends from the lower boundary of 30 hours, established for the South Portuguese coast (Almeida et al., 2012), to the upper limit of 96 hours (Martzikos et al., 2021). However, since the POT combinations analyzed included a minimum storm duration of 48 hours, adopting an independence interval shorter than this would lack physical consistency. Consequently, the lower boundary was fixed at 48 hours (2 days)."

3. **Since these parameters are inherently site-specific, a systematic evaluation of 45 POT parameter combinations was carried out in this study to identify the configuration that best captures morphologically significant events at the study site. Lines 119-120; Table 1: Table 1 shows that the mean significant wave height (Hs) for six selected years is very similar (1.00m - 1.11m). Does this limit the testing of the method under extremely variable climates?**

We acknowledge the reviewer's observation. While the mean Hs values are indeed similar across the six selected years — as they correspond to the same geographic location and therefore share a common regional wave climate — the percentile distribution and energy characteristics vary considerably between years. The primary objective of this study was to evaluate the method's sensitivity to inter-annual variability in energy distribution at a specific site, rather than to compare fundamentally different wave climates. Focusing on a single representative location allowed for a high-resolution assessment of event-based changes while maintaining a manageable computational cost and minimizes confounding factors associated with differences in regional oceanographic settings. We have clarified this in Section 2.2. "Hydrodynamic Forcings" of the revised manuscript, which now reads as follows: *"While mean H_s values were similar (1.00–1. 11 m), the most extreme waves (e.g. H_s 99th) showed greater variability, ranging from 2,89 m to 3,76 m (Table 1). This selection focuses on a single representative site to evaluate the methodology's sensitivity to inter-annual variability in wave energy distribution, rather than climatic shifts across different locations. This approach ensures consistency in regional characteristics while maintaining a manageable computational cost for high-resolution event-based analysis".*

4. **Lines 135-136; Line 576: A constant river discharge of 10 m^3/s is used in the model setup. However, in reality, storm events causing significant wave height changes often coincide with heavy rainfall and high river discharge. Neglecting the surge in discharge during storms might lead to a misinterpretation of the storm events and their driving mechanisms.**

The authors acknowledge the referees' concerns regarding the simplified initial conditions. The use of a constant river discharge in the idealized simulations was a deliberate methodological choice, consistent with established idealized modeling frameworks in coastal morphodynamics (e.g., Jiménez-Robles et al., 2016; Ruiz-Reina & López-Ruiz, 2021). In this context, the constant discharge allows us to isolate the morphological response driven specifically by wave-induced processes, minimizing the confounding influence of fluvial forcing on the results.

However, we believe that the application of the methodology to real-world scenarios, as discussed in the previous response and in the revised manuscript, addresses these concerns. In those cases, the bathymetries reflect natural sediment variability (including spatially distributed D_{50}), and the forcing inputs are based on empirical data, including complete tidal regimes, variable river discharges, and explicit wind forcing alongside buoy-derived wave data. Furthermore, the concurrent increase in river discharge during storm events is a physically relevant process (particularly in fluvially influenced systems such as the Guadiana estuary and the Punta Umbría Inlet) which is now explicitly accounted for in our real-world validation.

The results demonstrate that the methodology remains robust even when these additional environmental complexities are introduced. Since the effectiveness of the approach is captured in both controlled idealized cases and complex natural environments, we believe the current scope provides a comprehensive validation of its robustness.

To further clarify this point (and the related to the previous comment), we have added a discussion of these considerations in Section 6.3 (formerly Section 5.3) “Limitations and further improvements” , which now reads: *“Although the method was developed following established idealized frameworks (e.g., Jiménez-Robles et al., 2016; Ruiz-Reina & López-Ruiz, 2021), its successful validation in calibrated environments with real-world forcings, which include wind, variable river discharge, and full tidal regimes, addresses the applicability to complex coastal zones and supports the robustness of the methodology under more complex forcing conditions.”*

5. **Lines 210-213; Lines 588-590: This study is entirely based on an idealized numerical model. Although the authors acknowledge the lack of field data comparison in Section 5.3, without empirical data validation, the so-called "optimal POT parameter combination" (95th percentile, 4-day independence, etc.) might merely be an artifact of the specific model settings. It is suggested that the authors at least discuss the robustness of these optimal parameters if model settings (such as friction coefficients or diffusion coefficients) were to change.**

Following the reviewers’ recommendation, eight new simulations were conducted as a sensitivity analysis. Maintaining all other parameters constant, the uniform horizontal eddy viscosity (originally set to 2 m^2/s) was tested at values of 1 and 5 m^2/s. Additionally, two Chèzy roughness coefficients (60 and 70) were evaluated against the original value of 65. These four sensitivity scenarios were performed for two different experiments from the original study: (1) 1980–1981 and (3) 1999–2000.

After applying the methodology proposed in the paper, the matches obtained for the Traditional POT combination (T-POT, POT(95, 3, 12)) and the Optimal POT combination POT(95, 4, 6) were compared (Table 2). The results yielded identical match percentages in all cases, demonstrating the robustness of the model and the stability of the optimal parameters.

This information has been added to the Section 2.4 “Model setup and experimental design” in the revised manuscript, and the corresponding table has been included in the Supplementary Material (Table S4, Table 2 from the present document). The text included reads as follows: “*A sensitivity analysis was conducted through eight additional simulations to assess the robustness of the methodology with respect to key model parameters. While maintaining all other parameters constant, the uniform horizontal eddy viscosity was tested at values of 1 and 5 m^2/s, and two Chèzy roughness coefficients (60 and 70, in both directions) were evaluated for comparison with the original values. These four sensitivity scenarios were performed for two representative experiments (1980–1981 and 1999–2000). The match percentages obtained for both the T-POT and the optimal POT combination were identical across all sensitivity scenarios (Table S4), confirming that the identified optimal parameter combination is independent of these numerical settings.*”

Table 2. Match results obtained for the T-POT (POT(95,3,12)) and the Optimal POT combination (POT(95,4,6)), including the original simulation and sensitivity analyses of uniform horizontal eddy viscosity (ε) and Chèzy roughness coefficients.

			LWP-ME90		Hs-ME90		LWP-ME95		Hs-ME95	
			NCV	SCV	NCV	SCV	NCV	SCV	NCV	SCV
1980-1981	T-POT	**Original**	**49.4**	**55.8**	**34.1**	**32**	**65.5**	**82.5**	**53.4**	**55.6**
		ε=1	49.4	55.8	34.1	32	65.5	82.5	53.4	55.6
		ε=5	49.4	55.8	34.1	32	65.5	82.5	53.4	55.6
		Chèzy=60	49.4	55.8	34.1	32	65.5	82.5	53.4	55.6
		Chèzy=70	49.4	55.8	34.1	32	65.5	82.5	53.4	55.6
	Optimal POT combination	**Original**	**53.2**	**55.8**	**37.1**	**35.5**	**72.9**	**82.9**	**53.4**	**62.6**
		ε=1	53.2	55.8	37.1	35.5	72.9	82.5	53.4	62.6
		ε=5	53.2	55.8	37.1	35.5	72.9	82.5	53.4	62.6
		Chèzy=60	53.2	55.8	37.1	35.5	72.9	82.5	53.4	62.6
		Chèzy=70	53.2	55.8	37.1	35.5	72.9	82.5	53.4	62.6
1999-2000	T-POT	**Original**	**50.2**	**53.3**	**36.2**	**35**	**63**	**68.25**	**47**	**36.1**
		ε=1	50.2	53.3	36.2	35	63	68.25	47	36.1
		ε=5	50.2	53.3	36.2	35	63	68.25	47	36.1
		Chèzy=60	50.2	53.3	36.2	35	63	68.25	47	36.1
		Chèzy=70	50.2	53.3	36.2	35	63	68.25	47	36.1
	Optimal POT combination	**Original**	**53.5**	**56.7**	**51.1**	**48.1**	**66.5**	**72.4**	**63.3**	**56.4**
		ε=1	53.5	56.7	51.1	48.1	66.5	72.4	63.3	56.4
		ε=5	53.5	56.7	51.1	48.1	66.5	72.4	63.3	56.4
		Chèzy=60	53.5	56.7	51.1	48.1	66.5	72.4	63.3	56.4
		Chèzy=70	53.5	56.7	51.1	48.1	66.5	72.4	63.3	56.4

6. **Table 2; Lines 253-255: The independence criterion in Table 2 tests intervals of 2, 3, and 4 days. However, for certain storm clusters, the interval might be less than 2 days. Why were shorter intervals (e.g., 24 or 36 hours) not tested?**

The choice of the independence criterion from 2 days to 4 days is well-supported by the literature in different oceanic regions. According to Mathiesen et al. (1994), an interval of 2 to 4 days is generally sufficient to guarantee the independence of extreme events. This is consistent with Méndez et al. (2006), who identified 3 days as the optimal threshold for independence, and Luceño et al. (2006), who noted that while statistical fit may improve with 3 to 6 days, they also pointed out that longer intervals risk a significant loss of data. More recent studies, such as Almarshed (2025), also report that intervals between 1 and 4 days are common practice in POT analyses of extreme wave heights. This range was selected to maintain a balance between ensuring physical independence and preserving a robust sample size. Furthermore, since the POT combinations studied included a minimum storm duration of 48 hours, adopting an independence interval shorter than this would lack physical consistency.

7. **Lines 320-324: The method defines a "match" if the wave height is observed within 24 hours after a climatic event. This 24-hour time lag seems to lack a strong physical or statistical basis. The authors should provide a sensitivity analysis or cite relevant literature to support this specific timeframe.**

The authors understand the reviewer's concern regarding this decision. To justify the 24-hour time lag, a preliminary sensitivity test was conducted evaluating different intervals: no lag, 3, 12, 24, and 48 hours. The 24-hour window was selected as provided the best synchronization between climatic events and the morphological events, as evidenced by the alignment of event occurrences (e.g., the correspondence between 'red dots' and 'black dots' in Figures 4 and 5).

While the authors acknowledge the importance of sensitivity analyses, they believe that including the full results of this test would unnecessarily increase the length and complexity of the manuscript, which is already quite extensive. Nevertheless, the consistency of this timeframe is further supported by the results shown across the Supplementary Material (Figures S1–S10), where the 24-hour lag yields physically realistic and consistent morphological interpretations across all simulated years. This interval is also physically consistent with the morphodynamic response timescale of mesotidal wave-dominated systems, where significant net volumetric changes typically develop over periods of hours to tens of hours following the onset of energetic forcing conditions.

8. **Lines 420-425: The results show that in some cases, LWP misses certain events. In the Discussion section, it would be more balanced to point out that LWP serves as a complementary proxy to Hs for capturing directional events, rather than implying it can completely replace Hs. The current phrasing occasionally appears too dismissive of Hs.**

We thank the reviewer for this constructive observation. We agree that the manuscript should present LWP as a complementary proxy to Hs rather than as a complete substitute, and we have revised the text accordingly. We have added the following sentences to discussion Section 6.2 (formerly Section 5.2), "Main novelties and methodological advances"**:** "*It should be noted, however, that the superior performance of LWP does not preclude the utility of Hs as a morphological proxy. In coastal settings characterized by a low LvC index, where cross-shore processes dominate sediment transport, H_s remains a more accurate indicator of morphologically significant events, suggesting that LWP serves as a complementary proxy rather than a total replacement.*"

References used for Referee #1

Almarshed, B. F.: Optimizing threshold selection for accurate prediction of long-term extreme wave heights, Journal of Engineering Research (Kuwait), 13, 2965–2983, https://doi.org/10.1016/j.jer.2024.12.005, 2025.

García-de-Lomas, J., Payo, A., Cuesta, J. A., and Macías, D.: Morphodynamic study of a 2018 mass-stranding event at Punta Umbria Beach (Spain): Effect of Atlantic Storm Emma on Benthic Marine Organisms, J Mar Sci Eng, 7, https://doi.org/10.3390/jmse7100344, 2019.

Jiménez-Robles, A. M., Ortega-Sánchez, M., and Losada, M. A.: Effects of basin bottom slope on jet hydrodynamics and river mouth bar formation, J Geophys Res Earth Surf, 121, 1110–1133, https://doi.org/10.1002/2016JF003871, 2016.

López-Dóriga, U. and Ferreira, Ó.: Longshore and cross-shore morphological variability of a berm-bar system under low to moderate wave energy, J Coast Res, 33, 1161–1171, https://doi.org/10.2112/JCOASTRES-D-16-00050.1, 2017.

Luceño, A., Menéndez, M., and Méndez, F. J.: The effect of temporal dependence on the estimation of the frequency of extreme ocean climate events, Proceedings of the Royal Society A: Mathematical, Physical and Engineering Sciences, 462, 1683–1697, https://doi.org/10.1098/rspa.2005.1652, 2006.

Málvarez, G., Ferreira, O., Navas, F., Cooper, J. A. G., Gracia-Prieto, F. J., and Talavera, L.: Storm impacts on a coupled human-natural coastal system: Resilience of developed coasts, Sci. Total Environ., 768, 144987, https://doi.org/10.1016/j.scitotenv.2021.144987, 2021.

Mathiesen, M., Goda, Y., Hawkes, P. J., Mansard, E., Martín, M. J., Peltier, E., Thompson, E. F., and van Vledder, G.: Methodes conseillées pour 1'analyse des houles extreme, Journal of Hydraulic Research, 32, 803–814, https://doi.org/10.1080/00221689409498691, 1994.

Méndez, F. J., Menéndez, M., Luceño, A., and Losada, I. J.: Estimation of the long-term variability of extreme significant wave height using a time-dependent Peak Over Threshold (POT) model, J Geophys Res Oceans, 111, https://doi.org/10.1029/2005JC003344, 2006.

Mentaschi, L., Vousdoukas, M. I., Voukouvalas, E., Dosio, A., and Feyen, L.: Global changes of extreme coastal wave energy fluxes triggered by intensified teleconnection patterns, Geophys Res Lett, 44, 2416–2426, https://doi.org/10.1002/2016GL072488, 2017.

Pinson, P., Reikard, G., and Bidlot, J. R.: Probabilistic forecasting of the wave energy flux, Appl Energy, 93, 364–370, https://doi.org/10.1016/j.apenergy.2011.12.040, 2012.

Ruiz-Reina, A. and López-Ruiz, A.: Short-term river mouth bar development during extreme river discharge events: The role of the phase difference between the peak discharge and the tidal level, Coastal Engineering, 170, 103982, https://doi.org/10.1016/j.coastaleng.2021.103982, 2021.

Rusu, L.: The near future expected wave power in the coastal environment of the Iberian Peninsula, Renew Energy, 195, 657–669, https://doi.org/10.1016/j.renene.2022.06.047, 2022

Anonymous Referee #2

This paper introduces a novel methodology for identifying coastal morphological changes using Longitudinal Wave Power (LWP) as a proxy, moving beyond traditional significant wave height (Hs) approaches. The integration of LWP with optimized POT parameters represents a significant advancement over conventional Hs-based approaches. The paper is well-structured with clear methodology sections, comprehensive figures, and detailed supplementary materials. However, the paper still presents some weakness that need to be resolved. Please find below my detailed comments:

The authors sincerely thank Reviewer 2 for their careful reading and insightful comments on our manuscript. Following their guidance, we have significantly revised the manuscript and added a new section regarding its application to real-world scenarios. To address the concerns about the absence of field data, we have now implemented the methodology using real-world models of two different study areas along the South Atlantic coast of the Iberian Peninsula. These applications were carried out using previously calibrated and validated numerical models, whose calibration and validation were performed against real measured bathymetric data. This provides a meaningful empirical grounding for the methodology beyond the idealized framework, while also introducing real-world forcings including observed wave conditions, complete tidal regimes, and variable river discharges, and also different sediment grain sizes.

1. **The most significant limitation is the experiments and findings rely on idealized numerical simulations without comparison to observed coastal morphological data. While the authors acknowledge the difficulty in obtaining synchronized hourly resolution data, the lack of any field validation severely limits confidence in the methodology's real-world applicability.**

Following the reviewers' suggestions, a new section has been incorporated into the manuscript to present the application of the methodology to two real-world study areas. These applications were carried out using previously calibrated and validated numerical models, whose calibration and validation were performed against real measured bathymetric data. This provides a meaningful empirical grounding for the methodology beyond the idealized framework, while also introducing real-world forcings including observed wave conditions, complete tidal regimes, and variable river discharges, and also different sediment grain sizes. As shown in the revised manuscript, the new Section 5, "Application to real-world study areas", reads as follows:

"*The methodology was applied to two different real-world study areas: the Punta Umbría Inlet, following Zarzuelo et al. (2019) and the Guadiana estuary, following López-Ruiz et al. (2020). For both study cases, models were implemented in Delft3D and have been calibrated and validated against field-measured bathymetric surveys, providing continuous morphological simulations over real observed periods. For the Punta Umbría Inlet, the model spans from July 2014 to October 2015, with model data obtained at 3-hour intervals. For the Guadiana estuary, two separate simulations with hourly data were utilized: (1) from July 2016 to June 2017, and (2) from June 2017 to December 2018. This section presents the match results for each simulation using the two primary POT combinations: T-POT and Combination 11.*

5.1. Punta Umbría Inlet

The Punta Umbría Inlet (hereinafter PUI) consists of a NW-SE trending channel, 8 km in length and 0.5 km in width, with a maximum depth of -12 m MSL. Characterized as an ebb-tidal system, it features minor ebb channels, shoals, and frontal lobes. The model utilizes a spatially distributed D50 sediment grain size, ranging from 0.5 to 4 mm. This is defined via a grid-based input file to reflect the natural variability of the seabed. Due to long-standing navigational difficulties associated with shoal development, a jetty was constructed at the inlet, reaching -4 m MSL. The numerical setup and validation procedures follow Zarzuelo et al. (2019) in their entirety. A comprehensive description of the model performance is available in that study.

The control volume used to apply the methodology is located in the channel (Figure S11 from Supplementary Material). The match values obtained for the T-POT are 43.4% and 41.4% for the LWP-ME90 and LWP-ME95, respectively, and 42,7% and 45,1% for the Hs-ME90 and Hs-ME95, respectively. For the optimal combination (Combination 11, POT(95,4,6)), the match results for LWP increase to 47.4% (ME90) and 47.5% (ME95), while the Hs matches remain identical to those of the T-POT. This suggests that the Combination 11 improves upon the T-POT for LWP while maintaining the same accuracy for Hs.

5.2. Guadiana estuary

The numerical setup for the Guadiana estuary follows the configuration described in López-Ruiz et al. (2020), where a comprehensive description of the model's calibration and performance is available. The study area encompasses the ebb-tidal delta of the Guadiana River, located at the southern border between Spain and Portugal. The region is characterized by a semi-diurnal mesotidal regime, with a mean tidal range of 2 m. Similar to the PUI, the river mouth is stabilized by a jetty system, and the main channel undergoes periodic dredging to maintain navigability. Sediment distribution in the area exhibits the high variability typical of deltaic environments, with grain sizes ranging from fine to coarse sands. The model utilizes a spatially distributed D50 sediment grain size, ranging from 1 to 10 mm. This is defined via a grid-based input file to reflect the natural variability of the seabed.

Two simulations covering different periods are available for this study area, hereafter referred to as Guadiana 1617 (from July 2016 to June 2017) and Guadiana 1718 (from June 2017 to December 2018). The control volume used to apply the methodology is located in the ebb delta, within an area comparable to the one analyzed by Garel et al. (2019) to unravel the sediment transport patterns in the delta (Figure S12 from Supplementary Material).

For Guadiana 1617, the match values obtained for the T-POT are 63.5% and 62.9% for the LWP-ME90 and LWP-ME95, respectively, and 64.3% and 63.9% for the Hs-ME90 and Hs-ME95, respectively. For the Combination 11, the match results for LWP increase to 67.5% (ME90) and 67.9% (ME95), while the Hs matches remain identical to those of the T-POT.

For the Guadiana 1718 period, the T-POT achieved match values of 72.3% and 90.5% for LWP (ME90 and ME95, respectively), and 73.1% and 90.5% for Hs. The Combination 11 improved the LWP-ME90 match to 79% and the Hs-ME90 to 74.4%, while maintaining identical results for all ME95 events. Notably, almost all ME95 occurred during Storm Emma (February 2018), which heavily impacted the South Atlantic coast of the Iberian Peninsula (Málvarez et al. 2021)."

As demonstrated, the application to real-world scenarios confirms the robustness of the methodology. The optimal POT combination (Combination 11) consistently outperforms the T-POT across the three simulations analyzed regarding LWP matches. The single exception is the Guadiana 1718 case, where the dominance of a single extreme event (Storm Emma) concentrates nearly all ME95 events within a brief period, thereby limiting the discriminatory capacity of the LWP-based proxy under such specific conditions. This behavior is consistent with the role of the LvC index discussed in Section 6.1 of the revised manuscript (and further detailed in our response to Comment 1), reinforcing the complementary nature of LWP and Hs as morphological proxies. Moreover, the Hs related matches for the optimal POT combination are equal to the T-POT matches, with the exception of Guadiana 1718, where the match for Hs-ME90 shows an improvement over the T-POT.

Storm Emma (February 28 – March 5, 2018) was a severe Atlantic event that triggered extreme meteorological and oceanographic conditions across the southwestern Iberian Peninsula. It produced a 22-year record significant wave height of 7.27 m and raised sea levels to 4.12 m through a combination of low atmospheric pressure and spring tides. These forces caused profound morphodynamic changes, including dune erosion of 2.5 m and the modification of seabed elevation at depths as great as -10 m (García-de-Lomas, et al., 2019; Málvarez et al. 2021).

The Figures S11 and S12 from the Supplementary Material correspond to Figure 1 and Figure 2, respectively, from the attached document.

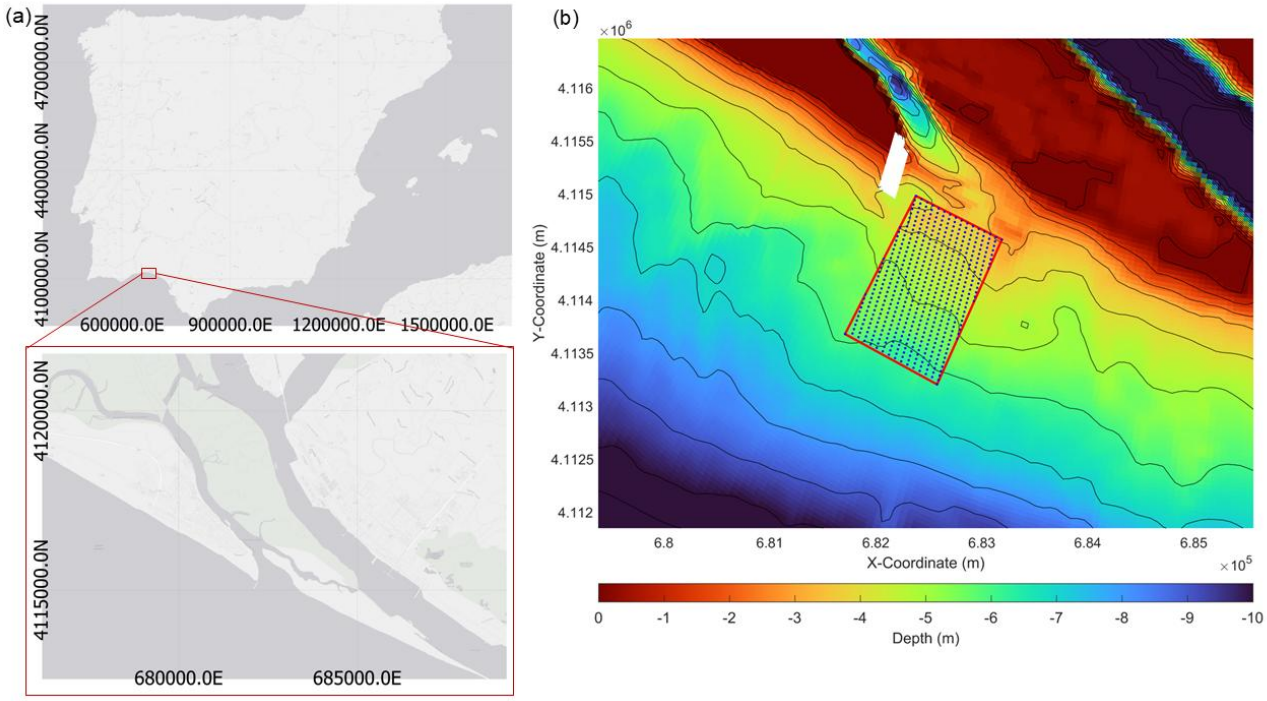

Figure 3. (a) Study area location in the Iberian Peninsula. (b) Control volume for the Punta Umbría Inlet shown on the actual bathymetry of the area. Bathymetric contours are represented every 1m, from 0 to -12 m MSL.

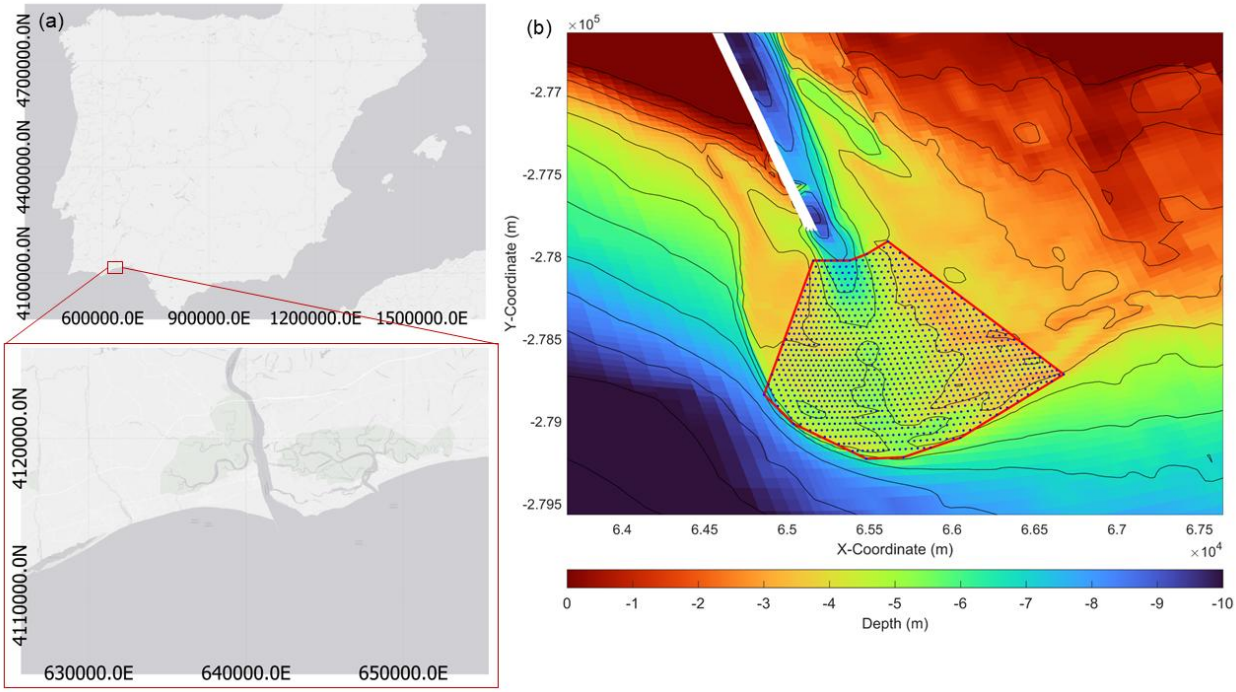

Figure 4. (a) Study area location in the Iberian Peninsula. (b) Control volume for the Guadiana Estuary shown on the actual bathymetry of the area. Bathymetric contours are represented every 1 m, from 0 to -12 m MSL.

2. **The study uses only a single sediment size (D50 = 1 mm), constant river discharge (10 m³/s), and a specific synthetic tidal regime (M2 and S2). These constraints limit application to complicated coastal environments. For example, the commonly used harmonic analysis for ocean tide generally include 8 major components. In addition, some sensitivity analysis for fine sands (D50 = 0.2-0.5 mm) or coarser sediments (D50 = 2-5 mm) may benefit.**

The authors acknowledge the referees' concerns regarding the simplified initial conditions. Regarding sediment grain size, following their guidance two additional simulations were conducted as a sensitivity analysis. Using Experiment 1 (1980–1981) as a baseline, we modified the original D_{50}=1mm in the simulation to D_{50} = 0.5 mm and D_{50} = 2mm.

Table 1. Match percentages obtained for different D_{50} values during the sensitivity analysis of Experiment 1 (1980–1981).

1980-1981		LWP-ME90		Hs-ME90		LWP-ME95		Hs-ME95	
		NCV	SCV	NCV	SCV	NCV	SCV	NCV	SCV
T-POT	**Original (D_{50} = 1mm)**	**49.4**	**55.8**	**34.1**	**32**	**65.5**	**82.5**	**53.4**	**55.6**
	D_{50} = 0.5 mm	38.4	68.8	28.4	45.1	41.2	88.7	39.8	61.8
	D_{50} = 2 mm	53.3	46,47	30.8	22.3	78.2	60.3	54.7	35.8
Optimal POT combination	**Original (D_{50} = 1mm)**	**53.2**	**55,78**	**37.1**	**35.5**	**72.9**	**82.5**	**53.4**	**62.6**
	D_{50} = 0.5 mm	38.4	68.8	31.6	49.5	41.2	88.7	39.8	69.2
	D_{50} = 2 mm	57.4	46.5	33.3	25.7	78.2	60.3	54.7	43.1

The results, presented in Table 1, show that the overall effectiveness of the methodology persists across different grain sizes. Specifically, a clear trend of improvement in the match related to LWP is observed in certain configurations, and the optimal POT combination consistently yields equal or higher match percentages compared to the traditional approach. Even having changes on the values according to the grain size, the overall match values are reasonably similar, with a difference that is lower than 10% for the majority of the tested conditions when referred to the original used value (D50 = 1 mm). However, given the current length of the manuscript and the addition of the new section featuring real-world data, we have decided to omit this specific information to maintain conciseness.

Regarding the tidal regime, the use of only two tidal components (M2 and S2) follows established approaches in the literature for morphodynamic simulations of river mouth systems (e.g., Jiménez-Robles et al., 2016; Ruiz-Reina & López-Ruiz, 2021). The primary objective was to reproduce the dominant tidal forcing in a controlled manner, rather than to replicate the full spectral complexity of a real tidal signal.

Similarly, the use of a constant river discharge in the idealized simulations was a deliberate methodological choice. In this context, the constant discharge allows us to isolate the morphological response driven specifically by wave-induced processes, minimizing the confounding influence of fluvial forcing on the results.

However, we believe that the application of the methodology to real-world scenarios, as discussed in the previous response and in the revised manuscript, addresses these concerns. In those cases, the bathymetries reflect natural sediment variability (including spatially distributed D_{50}), and the forcing inputs are based on empirical data, including complete tidal regimes, variable river discharges, and explicit wind forcing alongside buoy-derived wave data. Furthermore, the concurrent increase in river discharge during storm events is a physically relevant process —particularly in fluvially influenced systems such as the Guadiana estuary and the Punta Umbría Inlet — which is now explicitly accounted for in our real-world validation.

The results demonstrate that the methodology remains robust even when these additional environmental complexities are introduced. Since the effectiveness of the approach is captured in both controlled idealized cases and complex natural environments, we believe the current scope provides a comprehensive validation of its robustness.

To further clarify this point (and the related to the previous comment), we have added a discussion of these considerations in Section 6.3 (formerly Section 5.3) “Limitations and further improvements” , which now reads: *“Although the method was developed following established idealized frameworks (e.g., Jiménez-Robles et al., 2016; Ruiz-Reina & López-Ruiz, 2021), its successful validation in calibrated environments with real-world forcings, which include wind, variable river discharge, and full tidal regimes, addresses the applicability to complex coastal zones and supports the robustness of the methodology under more complex forcing conditions.”*

3. **Another problem is the exclusion of wind effects. The storm impacts on morphological changes are an important part of this paper but the contribution of winds seems totally ignored, which potentially weaken the value of these findings.**

We thank the reviewer for raising this point. Consistent with our previous responses, the exclusion of explicit local wind forcing from the idealized simulations was a deliberate methodological choice, consistent with established idealized morphodynamic modeling frameworks (see previous response) to avoid additional non-linearities, as local wind forcing would complicate the isolation of morphological responses driven purely by wave-induced processes.

This limitation is mitigated in the real-world applications presented in the new Section 5, where both models incorporate explicit wind forcing alongside buoy-derived conditions. Our results demonstrate that the methodology remains effective in both cases, suggesting that the presence of explicit wind forcing does not compromise the application or the reliability of the findings. Moreover, while the idealized model does not explicitly include local wind forcing, the wave conditions are derived from buoy data, which inherently capture the energy transferred by wind.

To further clarify this point (and the related to the previous comment), we have added a discussion of these considerations in Section 6.3 (formerly Section 5.3) “Limitations and further improvements” , as explained in the previous response.

4. **I am not sure about the definition of the CI. What is the reason for the 70-30 weighting? Was any optimization performed to determine these weights?**

Regarding the CI index, our objective was to prioritize the average performance of the metrics while still accounting for their variability across different wave climates.

The primary objective of the CI is to identify the POT combination that most effectively captures morphologically significant events across all simulated years. The mean match percentage is the most direct measure of this overall effectiveness and therefore receives the higher weight (70%). The standard deviation, in contrast, quantifies the variability of the match across different wave climates, which is a secondary but relevant consideration: a combination that performs well on average but inconsistently across years is less reliable than one that achieves a similarly high mean with lower variability. A weight of 30% was assigned to reflect this secondary role. Consequently, the dispersion remains a critical factor in identifying climates where the proxy performs more consistently (a behavior related to the LvC index explained in the response to question 6).

Furthermore, the 70-30 weighting is consistent with the trends observed in Figures 6 and 7, which demonstrate that this balance best represents the overall stability of the results across the tested scenarios. Finally, the application of the methodology to the real-world scenarios (new Section 5, question 1) confirms these findings, as the optimized POT combination identified by the CI yielded a higher match and superior performance, further validating it.

5. **I would recommend adding boundary conditions in the Fig. 1 to clearly illustrate their settings.**

The figure has been modified following the reviewer’s suggestion. The revised Figure 1 (Figure 3 from the present document) is as follows:

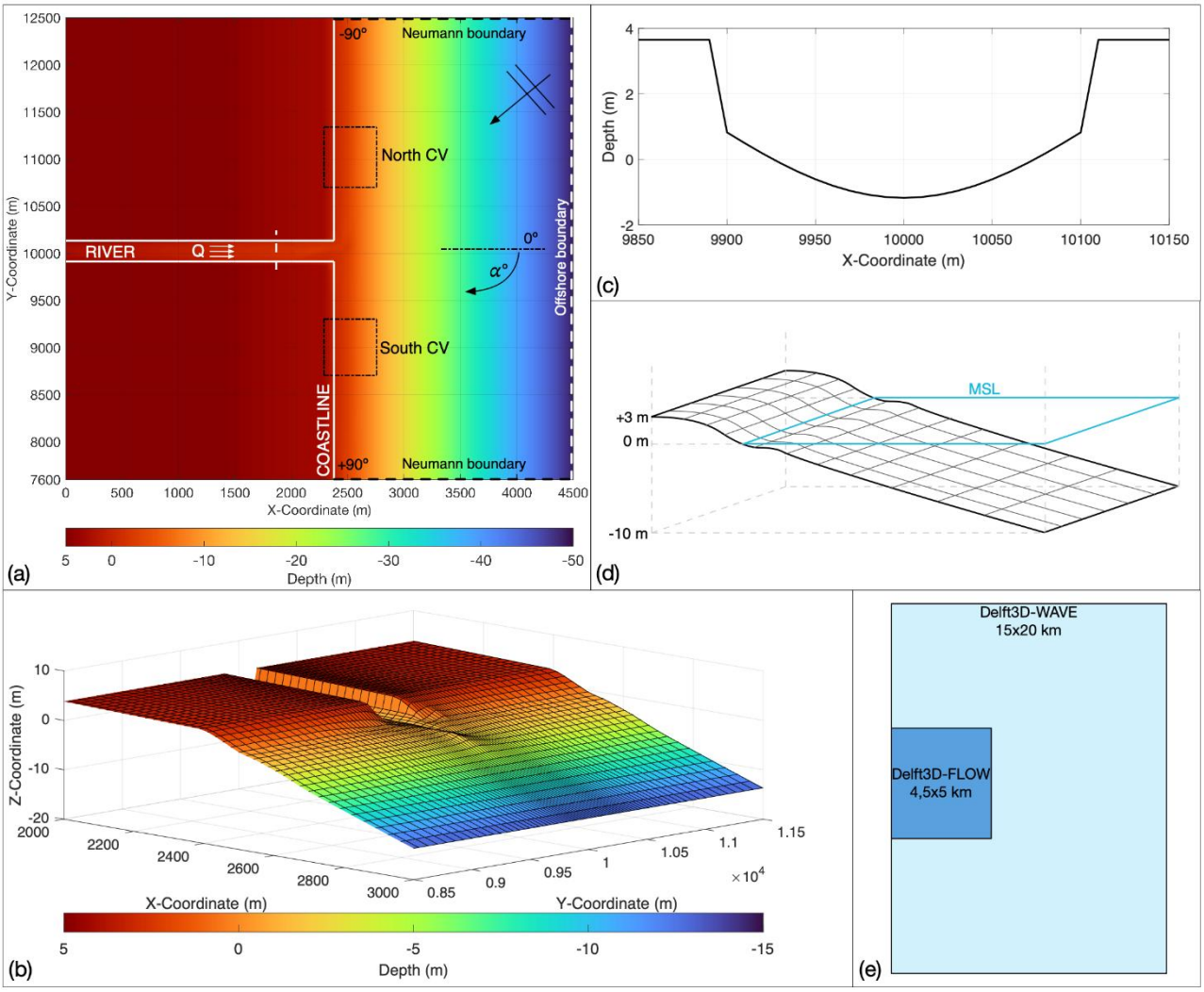

Figure 3 - Physical scenario: (a) and (b) depict the smoothed bathymetry (basic state) used for the simulations; (a) plan view where the dashed black line represents shore-normal incident waves, with positive (negative) values indicating waves coming from the South (North) part of the figure, and the white arrows on the river channel indicates the flow discharge (Q); (b) 3D view; (c) channel cross-section corresponding to the dashed white line position in (a); (d) representation of the surface (with variable grid) and the limits for the volume calculated in each control volume (CV) depicted in (a); and (e) the Delft3D-FLOW domain embedded into a larger Delft3D-WAVE domain; note that the FLOW domain is coupled with the WAVE domain.

6. **Although the mean significant wave heights for the six years are similar, Table 1 shows significant differences in total wave power (e.g., Exp 5 and Exp 6). Are these differences caused by storm frequency or duration? How might these variations in wave climate characteristics affect the applicability of the optimal POT parameters under different climate conditions?**

We acknowledge the reviewer's observation. The climate analysis (Table 1 of the manuscript) indicates that the differences in total wave power between experiments are driven by a combination of storm frequency and intensity, rather than a single factor or a simple linear relationship with the number of storm days.

Taking Experiments 5 (2010–11) and 6 (2019–20) as an illustrative example, Experiment 5 exhibits significantly higher energy levels (+104 kW/m) and more extreme peaks, with a Hs 99th percentile of 3.76 m compared to 3.33 m in Experiment 6. This higher total wave power is further explained by a

greater number of energetic events exceeding the 95th percentile threshold. A detailed breakdown of storm frequency and energy metrics for all experiments is provided in Table 1 of the manuscript.

We have clarified the difference between the inter-annual variability in Section 2.2. "Hydrodynamic Forcings" of the revised manuscript, which now reads as follows: "*While mean Hs values were similar (1.00–1.11 m), the most extreme waves (e.g. Hs 99th) showed greater variability, ranging from 2,89 m to 3,76 m (Table 1). This selection focuses on a single representative site to evaluate the methodology's sensitivity to inter-annual variability in wave energy distribution, rather than climatic shifts across different locations. This approach ensures consistency in regional characteristics while maintaining a manageable computational cost for high-resolution event-based analysis*".

Regarding the applicability of the optimal POT parameters, our results demonstrate that although the match percentages fluctuate depending on the year's energy (e.g., higher H_s match in Exp 5 vs. improved LWP match in Exp 6), the optimal combination (Combination 11) consistently outperforms the standard T-POT across all scenarios. This suggests that the methodology is robust to inter-annual climate variations at the site.

Moreover, to take into account the applicability of the optimal POT parameters under different climate conditions, the Longshore vs. Cross-shore index proposed by López-Dóriga and Ferreira (2017) (LvC index) was implemented. This index relates wave energy conditions to volumetric sediment changes to determine whether a storm event or coastal area is longshore-dominated or cross-shore-dominated. This information was incorporated into the present study in section 6.1 "The role of wave direction" (formerly Section 5.1) of the revised manuscript, reading as follows: "*Furthermore, by applying the LvC (Longshore vs. Cross-shore) index proposed by López-Dóriga and Ferreira (2017), it was found that the NCV exhibits a more cross-shore dominated in experiment 2 (1990-91) with an LvC=0.18, and in experiment 5 (2010-11) with LvC=0.01, both of which correspond to a higher H_s-match. Conversely, the SCV shows systematically higher LvC across most experiment, indicating a greater degree of longshore dominance, which corresponds with a higher LWP-match. The calculated LvC indices for all experiments and control volumes are provided in Table S5 of the Supplementary Material.*".

Table S5 from the Supplementary Material corresponds to Table 2 of the present document.

Table 2. LvC index calculated for each CV and for each experiment.

Year (Experiment)	NCV	SCV
1980-1981 (1)	0.25	0.30
1990-1991 (2)	0.18	0.60
1999-2000 (3)	0.85	0.66
2000-2001 (4)	0.38	0.44
2010-2011 (5)	0.01	0.40
2019-2020 (6)	0.17	0.75

7. **Lines 455-465 & Figures 8-9: The statistical analysis reveals that POT combinations with 48-hour minimum duration show drastically reduced performance. This suggests that morphologically significant events in your study area are characterized by short-lived, high-intensity impulses. How would this finding translate to regions with different storm characteristics, such as tropical cyclone environments where sustained wind conditions may persist for days?**

The authors acknowledge the concern regarding the generalization of the method. However, it should be noted that the methodology and the optimal POT parameters are calibrated for the wave climates observed along the Andalusian coast, which is characterized by an oceanic-influenced Mediterranean climate on its Atlantic side and a typical Mediterranean climate in the Mediterranean side. The Atlantic coast of Andalusia is characterized by a transitional oceanic-Mediterranean climate in which energetic storm events are typically short-lived and associated with high peak wave heights rather than sustained forcing over multiple days. In this context, requiring a minimum storm duration of 48 hours to define a POT event results in the exclusion of numerous short but morphologically significant events, thereby reducing the match between identified climatic events and observed morphological changes.

As stated by Almarshed (2025), POT parameters are context-specific and vary across different geographic regions. Therefore, when applying this method to areas characterized by tropical cyclone environments or sustained storm conditions, a site-specific re-optimization of the POT parameters would be necessary to capture the different temporal and intensity scales of those events.

In tropical cyclone environments, where sustained forcing may persist for several days, longer minimum duration thresholds would likely yield better performance, and a site-specific re-optimization of the POT parameters would be required. However, it is important to distinguish between the site-specificity of the optimal parameters and the generalizability of the methodological framework itself: the LWP-based POT approach proposed in this study is applicable to any coastal environment, provided that the POT parameters are calibrated locally using representative morphological and wave data

Overall, the paper represents good work that merits publication after major revisions.

References used for Referee #2

Almarshed, B. F.: Optimizing threshold selection for accurate prediction of long-term extreme wave heights, Journal of Engineering Research (Kuwait), 13, 2965–2983, https://doi.org/10.1016/j.jer.2024.12.005, 2025.

García-de-Lomas, J., Payo, A., Cuesta, J. A., and Macías, D.: Morphodynamic study of a 2018 mass-stranding event at Punta Umbria Beach (Spain): Effect of Atlantic Storm Emma on Benthic Marine Organisms, J Mar Sci Eng, 7, https://doi.org/10.3390/jmse7100344, 2019.

Jiménez-Robles, A. M., Ortega-Sánchez, M., and Losada, M. A.: Effects of basin bottom slope on jet hydrodynamics and river mouth bar formation, J Geophys Res Earth Surf, 121, 1110–1133, https://doi.org/10.1002/2016JF003871, 2016.

López-Dóriga, U. and Ferreira, Ó.: Longshore and cross-shore morphological variability of a berm-bar system under low to moderate wave energy, J Coast Res, 33, 1161–1171, https://doi.org/10.2112/JCOASTRES-D-16-00050.1, 2017.

Málvarez, G., Ferreira, O., Navas, F., Cooper, J. A. G., Gracia-Prieto, F. J., and Talavera, L.: Storm impacts on a coupled human-natural coastal system: Resilience of developed coasts, Sci. Total Environ., 768, 144987, https://doi.org/10.1016/j.scitotenv.2021.144987, 2021.

Ruiz-Reina, A. and López-Ruiz, A.: Short-term river mouth bar development during extreme river discharge events: The role of the phase difference between the peak discharge and the tidal level, Coastal Engineering, 170, 103982, https://doi.org/10.1016/j.coastaleng.2021.103982, 2021.

Anonymous Referee #3

This study proposes a novel methodology based on Longitudinal Wave Power (LWP) to identify coastal morphological changes, aiming to improve upon traditional approaches that rely solely on wave height (Hs). Through numerical simulations, the research demonstrates that the LWP-based method outperforms the Hs-based approach. The work is innovative and holds potential for coastal management applications. However, several details require further discussion and clarification. The following suggestions are provided to strengthen the manuscript:

The authors sincerely thank Reviewer 3 for their careful reading and insightful comments on our manuscript. Following their guidance, we have significantly revised the manuscript and added a new section regarding its application to real-world scenarios. To address the concerns about the absence of field data, we have now implemented the methodology using real-world models of two different study areas along the South Atlantic coast of the Iberian Peninsula. These applications were carried out using previously calibrated and validated numerical models, whose calibration and validation were performed against real measured bathymetric data. This provides a meaningful empirical grounding for the methodology beyond the idealized framework, while also introducing real-world forcings including observed wave conditions, complete tidal regimes, and variable river discharges, and also different sediment grain sizes.

1. **The study is based on idealized numerical simulations; however, the differences between an idealized coastal zone and real-world, complex topography are not discussed. Furthermore, the use of only six wave climate conditions may not adequately capture natural variability. It is necessary to discuss how these simplifications affect the generalizability of the conclusions. The authors could consider supplementing the analysis with additional climate scenarios or case studies for validation.**

Following the reviewers' suggestions, a new section has been incorporated into the manuscript to present the application of the methodology to two real-world study areas. These applications were carried out using previously calibrated and validated numerical models, whose calibration and validation were performed against real measured bathymetric data. This provides a meaningful empirical grounding for the methodology beyond the idealized framework, while also introducing real-world forcings including observed wave conditions, complete tidal regimes, and variable river discharges, and also different sediment grain sizes. As shown in the revised manuscript, the new Section 5, "Application to real-world study areas", reads as follows:

"*The methodology was applied to two different real-world study areas: the Punta Umbría Inlet, following Zarzuelo et al. (2019) and the Guadiana estuary, following López-Ruiz et al. (2020). For both study cases, models were implemented in Delft3D and have been calibrated and validated against field-measured bathymetric surveys, providing continuous morphological simulations over real observed periods. For the Punta Umbría Inlet, the model spans from July 2014 to October 2015, with model data obtained at 3-hour intervals. For the Guadiana estuary, two separate simulations with hourly data were utilized: (1) from July 2016 to June 2017, and (2) from June 2017 to December 2018. This section presents the match results for each simulation using the two primary POT combinations: T-POT and Combination 11.*

5.1. Punta Umbría Inlet

The Punta Umbría Inlet (hereinafter PUI) consists of a NW-SE trending channel, 8 km in length and 0.5 km in width, with a maximum depth of -12 m MSL. Characterized as an ebb-tidal system, it features minor ebb channels, shoals, and frontal lobes. The model utilizes a spatially distributed D50 sediment grain size, ranging from 0.5 to 4 mm. This is defined via a grid-based input file to reflect the natural variability of the seabed. Due to long-standing navigational difficulties associated with shoal development, a jetty was constructed at the inlet, reaching -4 m MSL. The numerical setup and validation procedures follow Zarzuelo et al. (2019) in their entirety. A comprehensive description of the model performance is available in that study.

The control volume used to apply the methodology is located in the channel (Figure S11 from Supplementary Material). The match values obtained for the T-POT are 43.4% and 41.4% for the LWP-ME90 and LWP-ME95, respectively, and 42,7% and 45,1% for the Hs-ME90 and Hs-ME95, respectively. For the optimal combination (Combination 11, POT(95,4,6)), the match results for LWP increase to 47.4% (ME90) and 47.5% (ME95), while the Hs matches remain identical to those of the T-POT. This suggests that the Combination 11 improves upon the T-POT for LWP while maintaining the same accuracy for Hs.

5.2. Guadiana estuary

The numerical setup for the Guadiana estuary follows the configuration described in López-Ruiz et al. (2020), where a comprehensive description of the model's calibration and performance is available. The study area encompasses the ebb-tidal delta of the Guadiana River, located at the southern border between Spain and Portugal. The region is characterized by a semi-diurnal mesotidal regime, with a mean tidal range of 2 m. Similar to the PUI, the river mouth is stabilized by a jetty system, and the main channel undergoes periodic dredging to maintain navigability. Sediment distribution in the area exhibits the high variability typical of deltaic environments, with grain sizes ranging from fine to coarse sands. The model utilizes a spatially distributed D50 sediment grain size, ranging from 1 to 10 mm. This is defined via a grid-based input file to reflect the natural variability of the seabed.

Two simulations covering different periods are available for this study area, hereafter referred to as Guadiana 1617 (from July 2016 to June 2017) and Guadiana 1718 (from June 2017 to December 2018). The control volume used to apply the methodology is located in the ebb delta, within an area comparable to the one analyzed by Garel et al. (2019) to unravel the sediment transport patterns in the delta (Figure S12 from Supplementary Material).

For Guadiana 1617, the match values obtained for the T-POT are 63.5% and 62.9% for the LWP-ME90 and LWP-ME95, respectively, and 64.3% and 63.9% for the Hs-ME90 and Hs-ME95, respectively. For the Combination 11, the match results for LWP increase to 67.5% (ME90) and 67.9% (ME95), while the Hs matches remain identical to those of the T-POT.

For the Guadiana 1718 period, the T-POT achieved match values of 72.3% and 90.5% for LWP (ME90 and ME95, respectively), and 73.1% and 90.5% for Hs. The Combination 11 improved the LWP-ME90 match to 79% and the Hs-ME90 to 74.4%, while maintaining identical results for all ME95 events. Notably, almost all ME95 occurred during Storm Emma (February 2018), which heavily impacted the South Atlantic coast of the Iberian Peninsula (Málvarez et al. 2021)."

As demonstrated, the application to real-world scenarios confirms the robustness of the methodology. The optimal POT combination (Combination 11) consistently outperforms the T-POT across the three simulations analyzed regarding LWP matches. The single exception is the Guadiana 1718 case, where the dominance of a single extreme event (Storm Emma) concentrates nearly all ME95 events within a brief period, thereby limiting the discriminatory capacity of the LWP-based proxy under such specific conditions. This behavior is consistent with the role of the LvC index discussed in Section 6.1 of the revised manuscript (and further detailed in our response to Comment 1), reinforcing the complementary nature of LWP and Hs as morphological proxies. Moreover, the Hs related matches for the optimal POT combination are equal to the T-POT matches, with the exception of Guadiana 1718, where the match for Hs-ME90 shows an improvement over the T-POT.

Storm Emma (February 28 – March 5, 2018) was a severe Atlantic event that triggered extreme meteorological and oceanographic conditions across the southwestern Iberian Peninsula. It produced a 22-year record significant wave height of 7.27 m and raised sea levels to 4.12 m through a combination of low atmospheric pressure and spring tides. These forces caused profound morphodynamic changes, including dune erosion of 2.5 m and the modification of seabed elevation at depths as great as -10 m (García-de-Lomas, et al., 2019; Málvarez et al. 2021).

The Figures S11 and S12 from the Supplementary Material correspond to Figure 1 and Figure 2, respectively, from the present document.

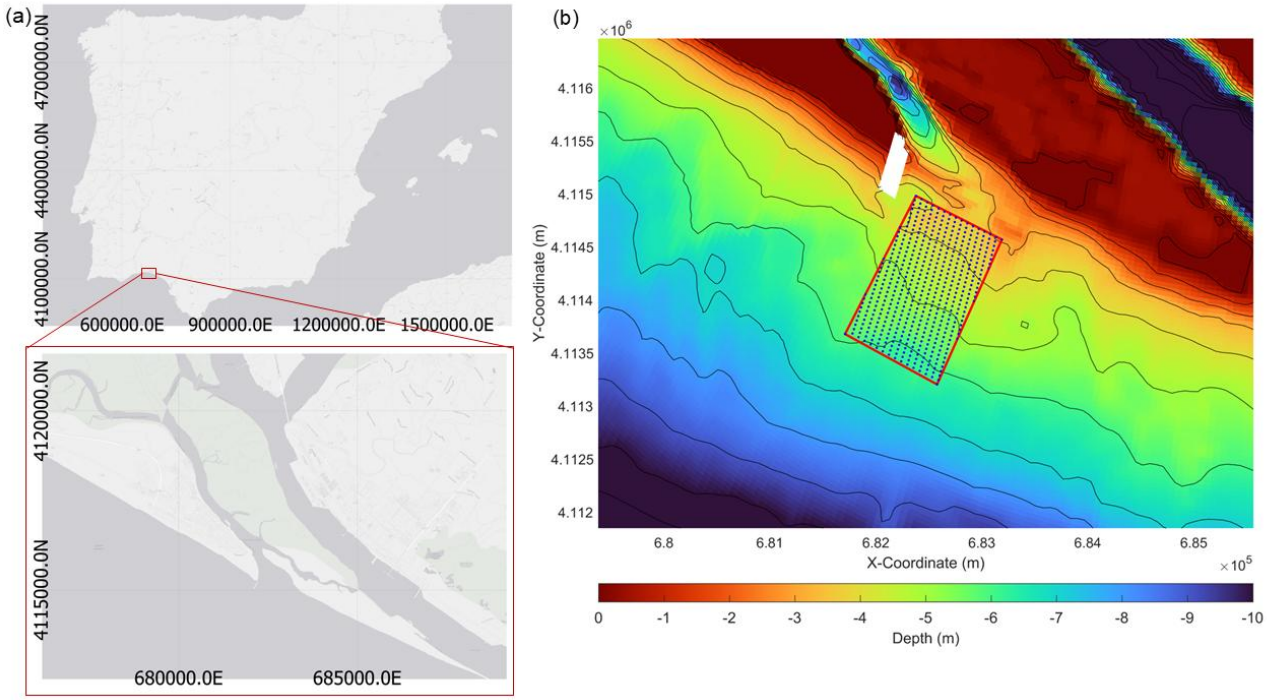

Figure 5. (a) Study area location in the Iberian Peninsula. (b) Control volume for the Punta Umbría Inlet shown on the actual bathymetry of the area. Bathymetric contours are represented every 1m, from 0 to -12 m MSL.

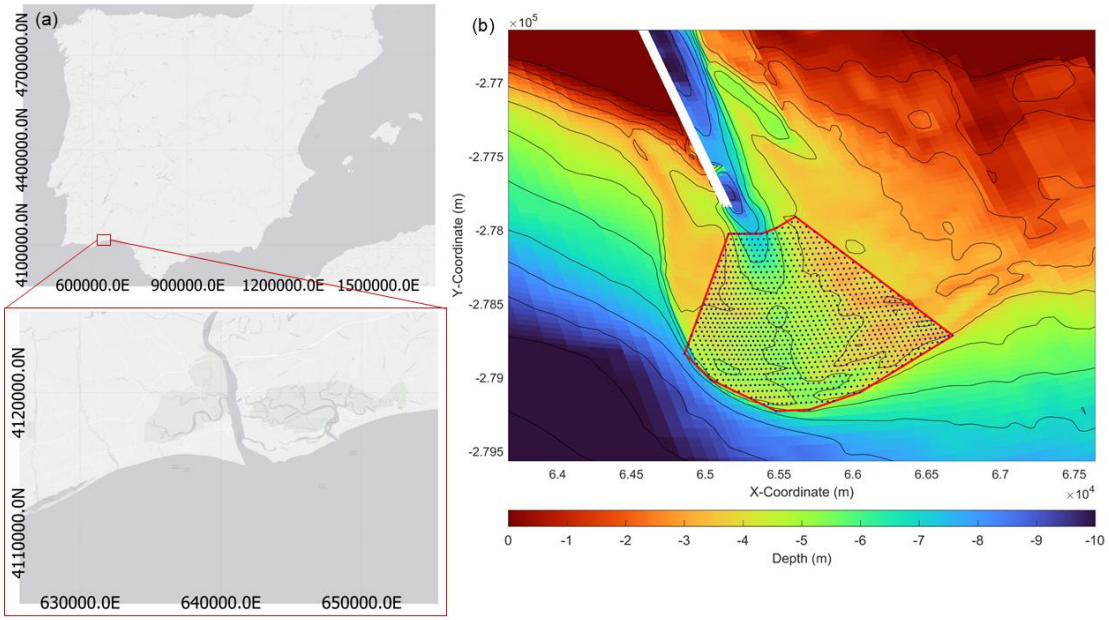

Figure 6. (a) Study area location in the Iberian Peninsula. (b) Control volume for the Guadiana Estuary shown on the actual bathymetry of the area. Bathymetric contours are represented every 1 m, from 0 to -12 m MSL.

2. **The study suggests that the optimal parameter combination (e.g., the 95th percentile threshold) may be site-specific, which is a key limitation. It is recommended that the authors include a discussion on sensitivity analysis—for example, exploring how the identification performance of this parameter set would change if key model parameters (such as bottom friction coefficient) were varied within reasonable ranges.**

Following the reviewers' recommendation, eight new simulations were conducted as a sensitivity analysis. Maintaining all other parameters constant, the uniform horizontal eddy viscosity (originally set to 2 m²/s) was tested at values of 1 and 5 m²/s. Additionally, two Chèzy roughness coefficients (60 and 70) were evaluated against the original value of 65. These four sensitivity scenarios were performed for two different experiments from the original study: (1) 1980–1981 and (3) 1999–2000.

After applying the methodology proposed in the paper, the matches obtained for the Traditional POT combination (T-POT, POT(95, 3, 12)) and the Optimal POT combination POT(95, 4, 6) were compared (Table 2). The results yielded identical match percentages in all cases, demonstrating the robustness of the model and the stability of the optimal parameters.

This information has been added to the Section 2.4 "Model setup and experimental design" in the revised manuscript, and the corresponding table has been included in the Supplementary Material (Table S4, Table 1 from the present document). The text included reads as follows: "*A sensitivity analysis was conducted through eight additional simulations to assess the robustness of the methodology with respect to key model parameters. While maintaining all other parameters constant, the uniform horizontal eddy viscosity was tested at values of 1 and 5 m²/s, and two Chèzy roughness coefficients (60 and 70, in both directions) were evaluated for comparison with the original values. These four sensitivity scenarios were performed for two representative experiments (1980–1981 and 1999–2000). The match percentages obtained for both the T-POT and the optimal POT combination*

were identical across all sensitivity scenarios (Table S4), confirming that the identified optimal parameter combination is independent of these numerical settings."

Table 1. Match results obtained for the T-POT (POT(95,3,12)) and the Optimal POT combination (POT(95,4,6)), including the original simulation and sensitivity analyses of uniform horizontal eddy viscosity (ε) and Chèzy roughness coefficients.

			LWP-ME90		Hs-ME90		LWP-ME95		Hs-ME95	
			NCV	SCV	NCV	SCV	NCV	SCV	NCV	SCV
1980-1981	T-POT	**Original**	**49.4**	**55.8**	**34.1**	**32**	**65.5**	**82.5**	**53.4**	**55.6**
		ε=1	49.4	55.8	34.1	32	65.5	82.5	53.4	55.6
		ε=5	49.4	55.8	34.1	32	65.5	82.5	53.4	55.6
		Chèzy=60	49.4	55.8	34.1	32	65.5	82.5	53.4	55.6
		Chèzy=70	49.4	55.8	34.1	32	65.5	82.5	53.4	55.6
	Optimal POT combination	**Original**	**53.2**	**55.8**	**37.1**	**35.5**	**72.9**	**82.9**	**53.4**	**62.6**
		ε=1	53.2	55.8	37.1	35.5	72.9	82.5	53.4	62.6
		ε=5	53.2	55.8	37.1	35.5	72.9	82.5	53.4	62.6
		Chèzy=60	53.2	55.8	37.1	35.5	72.9	82.5	53.4	62.6
		Chèzy=70	53.2	55.8	37.1	35.5	72.9	82.5	53.4	62.6
1999-2000	T-POT	**Original**	**50.2**	**53.3**	**36.2**	**35**	**63**	**68.25**	**47**	**36.1**
		ε=1	50.2	53.3	36.2	35	63	68.25	47	36.1
		ε=5	50.2	53.3	36.2	35	63	68.25	47	36.1
		Chèzy=60	50.2	53.3	36.2	35	63	68.25	47	36.1
		Chèzy=70	50.2	53.3	36.2	35	63	68.25	47	36.1
	Optimal POT combination	**Original**	**53.5**	**56.7**	**51.1**	**48.1**	**66.5**	**72.4**	**63.3**	**56.4**
		ε=1	53.5	56.7	51.1	48.1	66.5	72.4	63.3	56.4
		ε=5	53.5	56.7	51.1	48.1	66.5	72.4	63.3	56.4
		Chèzy=60	53.5	56.7	51.1	48.1	66.5	72.4	63.3	56.4
		Chèzy=70	53.5	56.7	51.1	48.1	66.5	72.4	63.3	56.4

3. **The use of constant river discharge and simplified tidal conditions may limit the applicability of the methodology to coasts dominated by variable riverine inputs and complex tidal dynamics. In real storm events, both factors can exhibit significant variability. The authors should address whether and how these simplifications influence the method's effectiveness in such environments.**

The authors acknowledge the referees' concerns regarding the simplified initial conditions. The use of a constant river discharge in the idealized simulations was a deliberate methodological choice, consistent with established idealized modeling frameworks in coastal morphodynamics (e.g., Jiménez-Robles et al., 2016; Ruiz-Reina & López-Ruiz, 2021). In this context, the constant discharge allows us to isolate the morphological response driven specifically by wave-induced processes, minimizing the confounding influence of fluvial forcing on the results.

However, we believe that the application of the methodology to real-world scenarios, as discussed in the previous response and in the revised manuscript, addresses these concerns. In those cases, the bathymetries reflect natural sediment variability (including spatially distributed D_{50}), and the forcing inputs are based on empirical data, including complete tidal regimes, variable river discharges, and explicit wind forcing alongside buoy-derived wave data. Furthermore, the concurrent increase in river

discharge during storm events is a physically relevant process (particularly in fluvially influenced systems such as the Guadiana estuary and the Punta Umbría Inlet) which is now explicitly accounted for in our real-world validation.

The results demonstrate that the methodology remains robust even when these additional environmental complexities are introduced. Since the effectiveness of the approach is captured in both controlled idealized cases and complex natural environments, we believe the current scope provides a comprehensive validation of its robustness.

To further clarify this point (and the related to the previous comment), we have added a discussion of these considerations in Section 6.3 (formerly Section 5.3) “Limitations and further improvements” , which now reads: *“Although the method was developed following established idealized frameworks (e.g., Jiménez-Robles et al., 2016; Ruiz-Reina & López-Ruiz, 2021), its successful validation in calibrated environments with real-world forcings, which include wind, variable river discharge, and full tidal regimes, addresses the applicability to complex coastal zones and supports the robustness of the methodology under more complex forcing conditions.”*

4. **Sediment grain size also influences coastal morphological changes. Conducting a sensitivity analysis with different sediment sizes could help broaden the applicability of the proposed method and clarify its constraints.**

The authors acknowledge the referees' concerns regarding the simplified initial conditions. Following their guidance two additional simulations were conducted as a sensitivity analysis. Using Experiment 1 (1980–1981) as a baseline, we modified the original D_{50}=1mm in the simulation to D_{50} = 0.5 mm and D_{50} = 2mm.

The results, presented in Table 2, show that the overall effectiveness of the methodology persists across different grain sizes. Specifically, a clear trend of improvement in the match related to LWP is observed in certain configurations, and the optimal POT combination consistently yields equal or higher match percentages compared to the traditional approach. Even having changes on the values according to the grain size, the overall match values are reasonably similar, with a difference that is lower than 10% for the majority of the tested conditions when referred to the original used value (D50 = 1 mm). However, given the current length of the manuscript and the addition of the new section featuring real-world data, we have decided to omit this specific information to maintain conciseness.

Table 2. Match percentages obtained for different D_{50} values during the sensitivity analysis of Experiment 1 (1980–1981).

1980-1981		LWP-ME90		Hs-ME90		LWP-ME95		Hs-ME95	
		NCV	SCV	NCV	SCV	NCV	SCV	NCV	SCV
T-POT	**Original (D_{50} = 1mm)**	**49.4**	**55.8**	**34.1**	**32**	**65.5**	**82.5**	**53.4**	**55.6**
	D_{50} = 0.5 mm	38.4	68.8	28.4	45.1	41.2	88.7	39.8	61.8
	D_{50} = 2 mm	53.3	46,47	30.8	22.3	78.2	60.3	54.7	35.8
Optimal POT combination	**Original (D_{50} = 1mm)**	**53.2**	**55. 8**	**37.1**	**35.5**	**72.9**	**82.5**	**53.4**	**62.6**
	D_{50} = 0.5 mm	38.4	68.8	31.6	49.5	41.2	88.7	39.8	69.2
	D_{50} = 2 mm	57.4	46.5	33.3	25.7	78.2	60.3	54.7	43.1

As explained above, our real-world application serves to bridge the gap between idealized modeling and complex coastal dynamics. The robustness of the methodology regarding sediment variability is further confirmed by them, which incorporate spatially distributed sediment data (see comment 1). This demonstrates that the LWP-based proxy remains effective even when subjected to the non-linearities and grain-size heterogeneity of natural coastal systems

5. **In Section 5.3 (Limitations and further improvements), limitations related to the Delft3D model configuration (e.g., neglecting wind effects, simplified initial bathymetry) are intermixed with those inherent to the LWP-based methodology itself. It is suggested that the authors clearly distinguish between limitations introduced by the numerical model and those intrinsic to the proposed LWP-POT identification method. This distinction would help readers better understand the different directions for future refinement.**

The authors appreciate this insightful comment. We agree that distinguishing between the limitations of the numerical setup (Delft3D) and those intrinsic to the LWP-based methodology is essential for future refinements.

To address the concerns regarding the numerical model's influence, we performed a new sensitivity analysis, as explained in the 2nd comment. The results demonstrate that the LWP methodology is highly robust and independent of specific numerical tuning parameters. While we acknowledge the inherent challenges associated with any numerical model, the setup used here has proven its reliability by successfully passing the sensitivity tests. Furthermore, the effectiveness of the model is confirmed by the successful calibration and validation of the real-world scenarios.

Regarding the intrinsic limitations of the LWP proxy, we have introduced a physical explanation based on the Longshore vs. Cross-shore (LvC) index (López-Dóriga & Ferreira, 2017) in the discussion section 6.1 "The role of wave direction". This index quantifies whether a storm event or a coastal area is dominated by longitudinal wave energy or cross-shore processes, and reads as follows: "*Furthermore, by applying the LvC (Longshore vs. Cross-shore) index proposed by López-Dóriga and Ferreira (2017), it was found that the NCV exhibits a more cross-shore dominated in experiment 2 (1990-91) with an LvC=0.18, and in experiment 5 (2010-11) with LvC=0.01, both of which correspond to a higher H_s-match. Conversely, the SCV shows systematically higher LvC across most experiment, indicating a greater degree of longshore dominance, which corresponds with a higher LWP-match. The calculated LvC indices for all experiments and control volumes are provided in Table S5 of the Supplementary Material.*"

Table S5 of Supplementary Material corresponds to Table 3 of present document.

Table 3. LvC index calculated for each CV and for each experiment.

Year (Experiment)	NCV	SCV
1980-1981 (1)	0.25	0.30
1990-1991 (2)	0.18	0.60
1999-2000 (3)	0.85	0.66
2000-2001 (4)	0.38	0.44
2010-2011 (5)	0.01	0.40
2019-2020 (6)	0.17	0.75

Following referee's advice, some changes were made to section 6.3 of the discussion "limitations and further improvements". The new section reads as follows: "*While the methodology offers several advances, it also has specific limitations that require further refinement. The use of deep-water variables, while providing flexibility and ease of application, may introduce uncertainties when applied to complex coastal sites with intricate bathymetry or varying nearshore wave conditions. This limitation can be particularly evident in areas where wave transformation between offshore and nearshore zones is complex and nonlinear, as observed by Loureiro et al. (2012b) in their study of geologically constrained morphological variability on embayed beaches.*

The robustness of the methodology is further supported by its transition from idealized configurations to real-world scenarios (Section 5). Although the method was developed following established idealized frameworks (e.g., Jiménez-Robles et al., 2016; Ruiz-Reina & López-Ruiz, 2021), its successful validation in calibrated environments with real-world forcings, which include wind, variable river discharge, and full tidal regimes, addresses the applicability to complex coastal zones and supports the robustness of the methodology under more complex forcing conditions.

This methodological approach differs from traditional H_s-based POT techniques used in coastal engineering and opens new research directions to verify its performance under different conditions. It represents the first application of LWP-based POT, making direct comparison with traditional H_s-based POT analyses challenging. The results demonstrate that climatic events can be effectively characterized through a composite LWP-based POT analysis, incorporating established parameters such as independence criteria and event duration. While the specific parameter combination identified appears robust for the detection of morphological events in the study area, it is likely to be site-dependent, requiring site-specific calibration in future applications. Future validation efforts may become feasible as emerging monitoring technologies (e.g., continuous video systems, high-resolution remote sensing) develop the capability to provide the required temporal resolution for morphological measurements, across a wider range of LvC conditions."

References used for Referee #3

García-de-Lomas, J., Payo, A., Cuesta, J. A., and Macías, D.: Morphodynamic study of a 2018 mass-stranding event at Punta Umbria Beach (Spain): Effect of Atlantic Storm Emma on Benthic Marine Organisms, J Mar Sci Eng, 7, https://doi.org/10.3390/jmse7100344, 2019.

Jiménez-Robles, A. M., Ortega-Sánchez, M., and Losada, M. A.: Effects of basin bottom slope on jet hydrodynamics and river mouth bar formation, J Geophys Res Earth Surf, 121, 1110–1133, https://doi.org/10.1002/2016JF003871, 2016.

López-Dóriga, U. and Ferreira, Ó.: Longshore and cross-shore morphological variability of a berm-bar system under low to moderate wave energy, J Coast Res, 33, 1161–1171, https://doi.org/10.2112/JCOASTRES-D-16-00050.1, 2017.

Málvarez, G., Ferreira, O., Navas, F., Cooper, J. A. G., Gracia-Prieto, F. J., and Talavera, L.: Storm impacts on a coupled human-natural coastal system: Resilience of developed coasts, Sci. Total Environ., 768, 144987, https://doi.org/10.1016/j.scitotenv.2021.144987, 2021.

Ruiz-Reina, A. and López-Ruiz, A.: Short-term river mouth bar development during extreme river discharge events: The role of the phase difference between the peak discharge and the tidal level, Coastal Engineering, 170, 103982, https://doi.org/10.1016/j.coastaleng.2021.103982, 2021.